Solid state systems for quantum information, Correction 7

Assistants : franco.depalma@epfl.ch, filippo.ferrari@epfl.ch

Exercise 1 : Driven linear and non-linear oscillator

The Cooper-pair box Hamiltonian

$$\hat{H}_{CPB} = 4E_C(\hat{n} - n_g)^2 - E_J \cos\left(\hat{\delta}\right), \tag{1}$$

in the so-called transmon limit, that is $E_J \gg E_C$, has low-lying levels with energy scale $\sqrt{8E_J E_C} \ll E_J$ much smaller than the amplitude of the cosine potential in the phase coordinate. Therefore, the phase δ is always close to zero when the system is in one of the low-lying energy levels, and we can perform Taylor expansion of the cosine as $-E_J \cos\left(\hat{\delta}\right) \approx \text{const} + E_J\frac{\hat{\delta}^2}{2} - E_J\frac{\hat{\delta}^4}{24}$. As the charge dispersion decreases exponentially with E_J/E_C, we neglect the charge offset n_g and reach the Hamiltonian

$$\hat{H}_T = 4E_C\hat{n}^2 + \frac{1}{2}E_J\hat{\delta}^2 - \frac{1}{24}E_J\hat{\delta}^4. \tag{2}$$

1. Treating the quartic term as a perturbation leads to a renormalized transition frequency ω, as well as a renormalized anharmonicity α. Show that the Hamiltonian in its second quantized form can be written as:

   $$\hat{H} = \hbar\left(\omega\hat{a}^\dagger\hat{a} + \frac{1}{2}\alpha\hat{a}^{\dagger 2}\hat{a}^2\right). \tag{3}$$

   What is the expression of the resonance frequency ω and the anharmonicity α?

2. We will take typical values for a transmon of $\omega/(2\pi) = 6$ GHz, and anharmonicity of $\alpha/(2\pi) = -300$ MHz. In order to demonstrate that such non-linear oscillator can be operated as an effective two-level system, i.e. a qubit, we study the time-evolution under the influence of a driving field. We model this drive as a pulse with a Gaussian envelope of the form $H_1 = \hbar A_0 e^{(-t/\tau)^2}\left(ae^{i\omega_d t} + a^\dagger e^{-i\omega_d t}\right)$, with $\tau = 5$ ns. The file Rabi_pulses-Questions.ipynb on Moodle provides a template on how to proceed.

   Define the Hamiltonian operator, and plot the evolution of the populations of the ground state and the first excited state over time, assuming an amplitude $A_0/(2\pi) \in \{0.18, 0.4\}$ GHz.

3. Plot the average number of excitations $\langle n\rangle = \langle a^\dagger a\rangle$ in the system at the end of the pulse versus the pulse amplitude. What do you observe?

   Hint: the qutip "mesolve" (master equation solver) function takes as parameters, in order, the Hamiltonian, the initial vector, the collapse operators (which we do not use in this exercise, thus pass "[]" as an argument), a list of operators for which to return the expectation value (if the list is empty, the function returns the the state vector), and additional parameters that one can sweep in the Hamiltonian.

4. Perform the same drive on a linear system, i.e. $\alpha = 0$. What qualitative change do you observe? Compare the final number of excitations in the two systems.

5. For a drive amplitude of $A_0/(2\pi) = 0.18$ GHz, plot the occupation probability in the Fock levels $0, 1, ...$ Discuss the state obtained in both cases.

Solution 1 :

1. Solved at the blackboard during the exercise sheet. See also "Notes - Lecture 5". A more detailed handwritten solution will be also uploaded.

2. The time evolution of the occupation probability of the first two levels of the transmon during the pulse is plotted in Fig. 1 for an amplitude of 0.18 GHz, where we see that the qubit smoothly transitions from the ground state to the first excited state. For a larger amplitude of 0.4 GHz, we notice that the probability to find the qubit excited decreases again after reaching its maximum, and the qubit can even return back to the ground state, see Fig. 2.
   Note: The sum of the two curves in Fig. 2 is slightly smaller than 1 during the pulse. When applying a strong pulse (A_0 approaches the frequency of the qubit ω), the ground and excited state of the qubit are not eigenstates of the driven system anymore, therefore the returned expectation values $\langle g \rangle$, $\langle e \rangle$ are not accurately monitoring the qubit populations during the pulse. Once the pulse is complete, the sum of the two curves is very close to 1, thus the qubit remains in its lowest two levels in good approximation.

3. As we increase the amplitude of the pulse, we observe an oscillatory behavior in the number of excitations in the system, see Fig. 3. Note that we never have more than one excitation in the system.

4. For a linear system with $\alpha = 0$, one notices that the system does not remain in the lowest two levels any longer, and thus cannot be considered a qubit, see Fig. 4 for the equivalent of Fig. 2 without nonlinearity. If one plots the average occupation i.e., the expectation of the number operator $n = a^\dagger a$, and contrasts it with the Rabi oscillations obtained in Fig. 3, we get Fig. 5. We see that the system grows to having more than one excitation on average, quadratically with the pulse amplitude (the deviation at large amplitude is caused by our cropping of the Hilbert space to 8 states).

5. The occupation probabilities of the various Fock levels for the linear and non-linear systems are plotted in Fig. 6. In the linear case, we obtain a coherent state with nearly perfect fidelity while we reach the first excited state with about 0.7% infidelity in the case of the transmon.
   Note 1: that typically one would consider a rotating frame (see also problem 2), where the atomic frequency is set to zero. This allows to obtain the same results with a coarser discretization in time as long as all frequencies are adapted to that rotating reference frame (try $\omega = 0$ in the python code).
   Note 2: The qubit approximation, in which the population remains in the lowest two levels, is valid only if the pulse bandwidth is small compared to the anharmonicity. Try decreasing τ in the code (thus increasing the bandwidth of the pulse in frequency domain) and see the effects yourself.

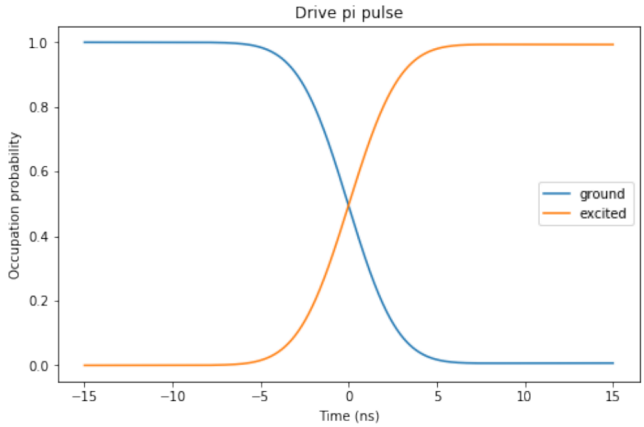

Figure 1: Time evolution of the occupation probability of the first two levels of the transmon during the pulse, for an amplitude of 0.18 GHz.

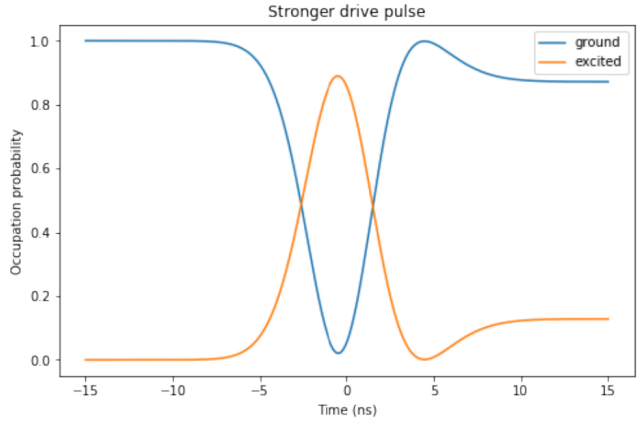

Figure 2: Time evolution of the occupation probability of the first two levels of the transmon during the pulse, for a larger amplitude of 0.4 GHz.

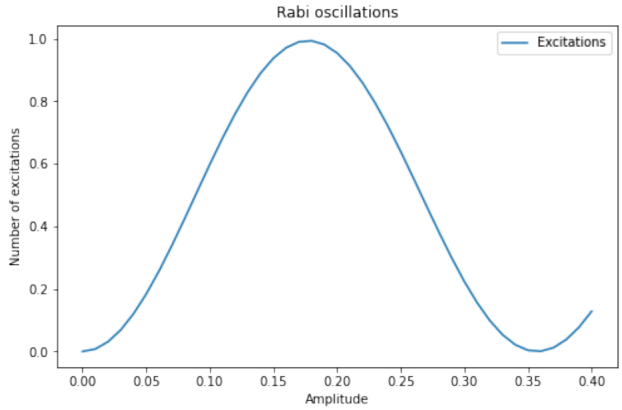

Figure 3: Rabi oscillations in the average number of excitations of the transmon versus the amplitude of the driving pulse.

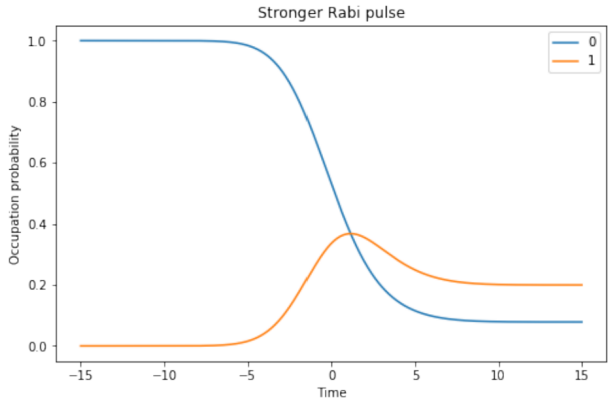

Figure 4: Time evolution of the occupation probability of the first two levels of a linear system during the pulse, for an amplitude of 0.4.

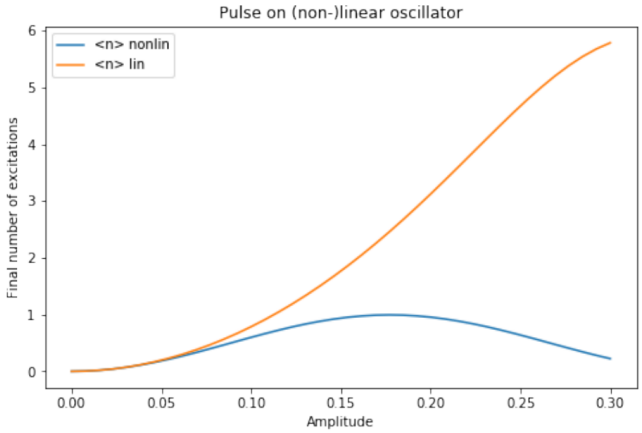

Figure 5: Final number of excitation $\langle n \rangle$ in a linear resonator, versus the pulse amplitude, contrasted to the Rabi oscillations of the first excited level σ_{ee} of a transmon qubit.

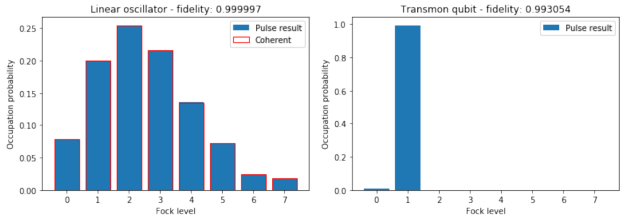

Figure 6: Occupation probability in the various Fock levels for the linear and non-linear systems.

Exercise 2 : Ramsey interferometry

The method of Ramsey interferometry is a widely used method in atomic clocks, modern atom interferometers and quantum logic gates. It allows precise measurement of the phase of a quantum state. We can illustrate the procedure for Ramsey interferometry using the following circuit diagram:

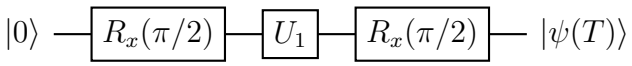

We prepare the qubit in state $|0\rangle$ and then rotate it into the superposition of $|0\rangle$ and $|1\rangle$ states using the gate $R_x(\pi/2)$, where $R_x(\theta) = e^{-i\theta\sigma_x/2}$, rotates the qubit by the angle θ around the x axis of the Bloch sphere (and similarly for $R_z(\theta) = e^{-i\theta\sigma_z/2}$). The qubit is then allowed to evolve freely for time T, and this is shown as gate U_1. In our case, the qubit is placed in a (time-varying) magnetic field $B(t)$, such that the energies of the two qubit states are split by $g\mu_B B(t)$, with g the electron g-factor, μ_B the Bohr magneton. Setting the energy of the lower state to 0, the Hamiltonian that governs the qubit's free evolution is given by $H = g\mu_B B(t)\,|1\rangle\langle 1|$. Given this, U_1 corresponds to $R_z\left(\int_0^T \frac{g\mu_B}{\hbar} B(t')\right)$. After the free evolution the qubit is rotated again using $R_x(\pi/2)$ to the state $|\psi(T)\rangle$ and is measured in the computational basis.

1. Draw the state after each step of the circuit diagram on a Bloch sphere. Do this for $U_1 = R_z(0)$ and $U_1 = R_z(\pi)$. Can you see the oscillation of $P_0(T) = |\langle 0|\psi(T)\rangle|^2$ with varying θ in $U_1 = R_z(\theta)$?

2. Calculate the probability of finding the qubit in state $|0\rangle$: $P_0(T) = |\langle 0|\psi(T)\rangle|^2$.
   Hint: $\exp\left(i\theta\sigma_{x/z}\right) = \mathbb{1}\cos\theta + i\sigma_{x/z}\sin\theta$.

3. We now want to investigate the effect of a noisy classical magnetic field. We will first assume $B(t)$ is constant for the duration of the experiment but upon repetition of the experiment takes on different, random values. We then can calculate the expectation value of observables over the ensemble average of magnetic field values. Assume $B(t) = B$ where B is a time-independent Gaussian random variable, with mean B_0 and variance B_1^2. Find $\langle P_0(T)\rangle$, where the brackets $\langle\ \rangle$ indicate the expectation value of the random variable.
   Hint: Recall that a Gaussian of a random variable X with mean μ and variance σ^2 is given by $\langle e^{-iXt}\rangle = e^{-i\mu t}e^{-\sigma^2 t^2/2}$.

Solution 2 :

For this problem we will consider the spin states of an electron as a qubit, and show how coherence of this qubit is affected by classical magnetic field noise that alters the energy difference between the two spin states. We introduce Ramsey interferometry, which allows one to measure effects of such dephasing. Let us denote electron's two spin states as $|0\rangle$ and $|1\rangle$. When the electron is placed in a (time-varying) magnetic field $B(t)$, the energies of the two qubit states are split by $g\mu_B B(t)$, with g the electron g factor, μ_B the Bohr magneton. Setting the energy of the lower state to 0, the Hamiltonian that governs the qubit's free evolution is given by $H = g\mu_B B(t)\,|1\rangle\langle 1|$.

1. First case: $U_1 = R_z(0)$.
   We start in the initial state $|0\rangle$. The first gate $R_x(\pi/2)$, will rotate the state around the $\hat{x}$

axis by $\pi/2$. The second gate $R_z(0)$ will do no operation on the state. The last gate, $R_z(\pi/2)$, will apply another rotation by $\pi/2$ around the $\hat{x}$ axis to the state $|1\rangle$.
Second case: $U_1 = R_z(\pi/2)$.
We start in the initial state $|0\rangle$. The first gate $R_x(\pi/2)$, will rotate the state around the $\hat{x}$ axis by $\pi/2$. The second gate $R_z(\pi)$ will rotate the state along the $\hat{z}$ axis by π. The last gate, $R_z(\pi/2)$, will apply another rotation by $\pi/2$ around the $\hat{x}$, which will this time rotate the state back to the ground state $|0\rangle$.
For different values of θ we can expect to see an oscillation in the probability $P_0(T) = |\langle 0|\psi(T)\rangle|^2$. This is better grasps by the series of three schematics below.

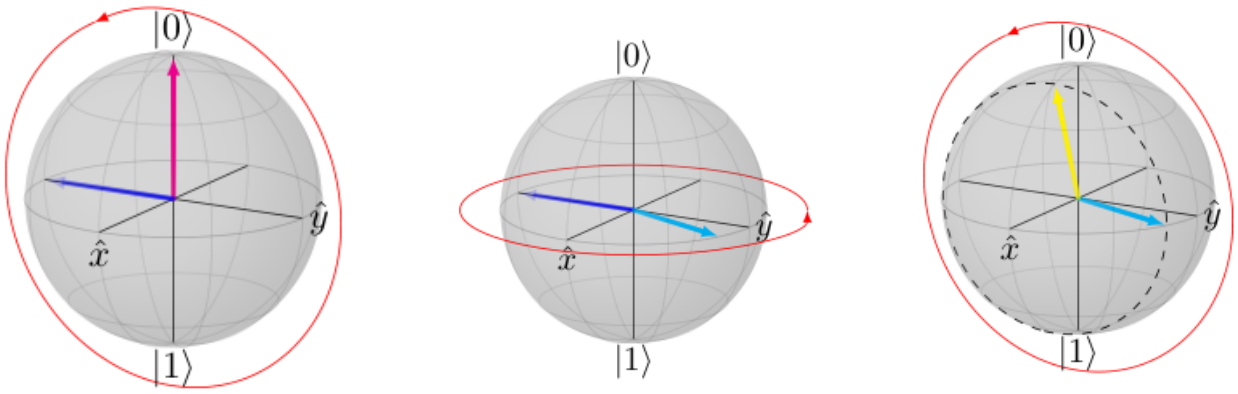

Figure 7: **Ramsey procedure.** Left: We start by doing a $\pi/2$ rotation along the $\hat{x}$ axis. Middle: We do a rotation along $\hat{z}$ by an angle θ. Right: We apply another $\pi/2$ rotation along the $\hat{x}$ axis. The state will end up between $|0\rangle$ and $|1\rangle$ depending on the value of θ.

2. Let's now get the previous result analytically by applying the gates one by one by using the identity given in the hint.
The first gate $R_x(\pi/2)$ will perform the following operation:

$$R_x(\pi/2)\,|0\rangle = (\cos(\pi/4)\,\mathbb{1} - i\sin(\pi/4)\sigma_x)\,|0\rangle = \frac{1}{\sqrt{2}}(|0\rangle - i\,|1\rangle). \tag{4}$$

The second gate $U_1 = R_z(\theta)$ will perform the following operation:

$$R_z(\theta)\frac{1}{\sqrt{2}}(|0\rangle - i\,|1\rangle) = \frac{1}{\sqrt{2}}(\cos(\theta/2)\mathbb{1} - i\sin(\theta/2)\sigma_z)(|0\rangle - i\,|1\rangle) \tag{5}$$

$$= \frac{1}{\sqrt{2}}(|0\rangle - ie^{i\theta}\,|1\rangle) \tag{6}$$

Finally the third gate, $R_x(\pi/2)$, will perform the following operation:

$$R_x(\pi/2)\frac{1}{\sqrt{2}}(|0\rangle - ie^{i\theta}\,|1\rangle) = \frac{1}{2}(|0\rangle - i\,|1\rangle - ie^{i\theta}(-i\,|0\rangle + |1\rangle)) \tag{7}$$

$$= \frac{1}{2}((1 - e^{i\theta})\,|0\rangle - i(1 + e^{i\theta})\,|1\rangle) = |\psi(T)\rangle \tag{8}$$

The probability of $P_0(T)$ is then

$$P_0(t) = |\langle 0|\psi(t)\rangle|^2 = \sin^2\theta/2 = \frac{1}{2}[1-\cos\theta] = \frac{1}{2}\left[1-\cos\left(\int_0^T \frac{g\mu_B B(t')}{\hbar}dt'\right)\right]. \quad (9)$$

3. We are interested in the following expectation value:

$$\begin{aligned}\langle P_0(T)\rangle &= \frac{1}{2}\left[1-\frac{1}{2}\left(\left\langle e^{i\frac{g\mu_B}{\hbar}BT}\right\rangle + \left\langle e^{-i\frac{g\mu_B}{\hbar}BT}\right\rangle\right)\right] \\ &= \frac{1}{2}\left[1-\frac{1}{2}\left(e^{-i\frac{g\mu_B}{\hbar}B_0T-\left(\frac{g\mu_B}{\hbar}\right)^2T^2B_1^2/2} + e^{+i\frac{g\mu_B}{\hbar}B_0T-\left(\frac{g\mu_B}{\hbar}\right)^2T^2B_1^2/2}\right)\right] \\ &= \frac{1}{2}\left[1-e^{-\left(\frac{g\mu_B B_1}{\hbar}\right)^2T^2/2}\cos\left(\frac{g\mu_B}{\hbar}B_0T\right)\right]\end{aligned} \quad (10)$$

Note the signal is periodic with B_0, and this periodic dependence is often used to determine the value of B_0 in experiments. The variance of the magnetic field B_1^2 leads to a decay of the periodic behaviour in a time-scale that is characterized by $T_2^\star = \frac{\hbar}{g\mu_B B_1}$.
It is also worth thinking about how different B values change the picture in the Bloch sphere, previously we had stated that B and T determine the angle of precession of the state vector in the equatorial plane. In the Bloch sphere illustrated below (blue state showing the state before the free evolution and cyan states showing the state after the free evolution), we show three different values of the state vector for different values of B for the same T (Fig. 9).

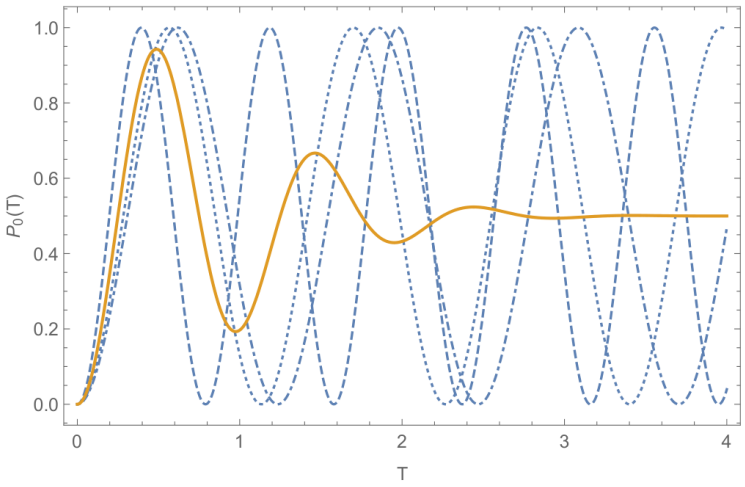

Figure 8: An illustration of different realizations of $P_0(T)$. The blue curves (dashed, dotted, dotted-dashed) illustrates P0(T) for 3 specific realizations of B. We pick B to be a random variable such that $g\mu_B B_0/\hbar = 2\pi$ and $g\mu_B B_1/\hbar = 1$. Physically this corresponds to completing the experiment (that samples all T) before B changes, but upon repetition of the experiment (say the next day) we find B has changed to a different realization. Averaging the signal from many such experiments then leads to the yellow thick line which has the shape given by $0.5\left(1-e^{-T^2/2}\cos 2\pi T\right)$. If the experiment relies on many repetitions of the experiment to obtain each point, and if we assume B changes on a timescale that is slightly longer than each such repetition, the experiment would only yield the yellow curve.

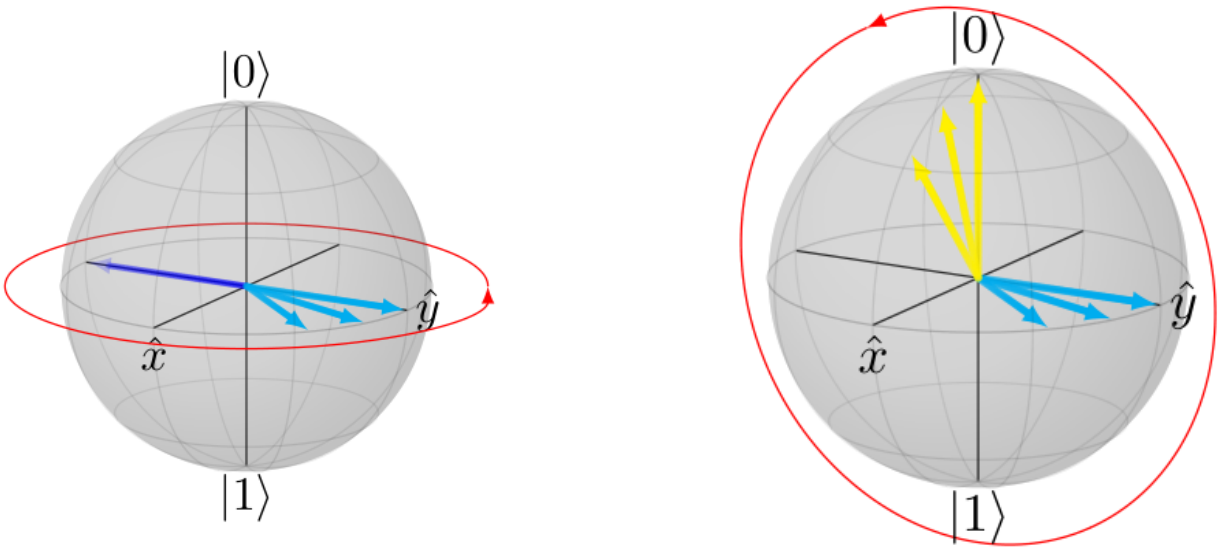

Figure 9: **Ramsey procedure in the presence of noise.** Left: After the $\pi/2$ pulse from the ground state we end up to the blue Bloch vector. Due to the noise in the magnetic field, the free evolution (cyan vectors) does not depend on time only anymore, but also on the amplitude of the noise in B. For this reason the quantum state during the free evolution can end up anywhere in the equator of the Bloch sphere. In this figure, we picture it by drawing three different cyan Bloch vectors. Right: after the second $\pi/2$ pulse, now due to the noise, we may get any of the three yellow vectors.

Exercise 3 : Circuit QED Hamiltonians in First Quantization

In this computational exercise we are going to build up the main Hamiltonians seen in the lecture notes from a different point of view. We will focus on the quantized LC circuit, whose Hamiltonian is given by

$$\hat{H} = \frac{\hat{Q}^2}{2C} + \frac{\hat{\Phi}^2}{2L}, \tag{11}$$

being $\hat{Q}$ and $\hat{\Phi}$ the charge and flux operators respectively, and C and L the capacitance and the inductance of the circuit, respectively. We will also focus on the transmon qubit, whose Hamiltonian reads instead

$$\hat{H} = 4E_C\hat{n}^2 - E_J\cos\hat{\phi} \tag{12}$$

where $\hat{n}$ and $\hat{\phi}$ are the charge number and phase operators, respectively, while E_C and E_J are the charging and Josephson energies, respectively. We assume zero offset charge n_g for simplicity.

1. We introduce the charge number and phase operators for the LC circuit

$$\hat{n} = \hat{Q}/2e, \qquad \hat{\phi} = (2\pi/\Phi_0)\hat{\Phi}, \tag{13}$$

being e the electron charge and $\Phi_0 = h/2e$ the magnetic flux quantum. From now one, we assume $\hbar = e = 1$. We also introduce the charging and the inductive energies as $E_C = 1/2C$ and $E_L = 1/4L$. Rewrite Eq. (11) in terms of $\hat{n}$, $\hat{\phi}$, E_C and E_L.

2. Expand $\hat{n}$ and ϕ in terms of creation and annihilation operators

$$\hat{\phi} = \left(\frac{2E_C}{E_L}\right)^{1/4} (\hat{a} + \hat{a}^\dagger), \qquad \hat{n} = \frac{i}{2}\left(\frac{E_L}{2E_C}\right)^{1/4} (\hat{a}^\dagger - \hat{a}). \tag{14}$$

Show that this choice diagonalizes the Hamiltonian. Write the eigenenergies in terms of E_C and E_L. This is the well known Second Quantization procedure.

3. We now compute eigenstates and eigenenrgies of Eq. (11) in First Quantization. Since number and phase operators are canonically conjugate variables, we can express $\hat{n}$ in the ϕ-basis as $\hat{n} = -i\partial/\partial\phi$. This allows us to write an Hamiltonian in the ϕ-basis only, $\mathcal{H} = T(\phi) + V(\phi)$. Using the central difference approximation scheme, write $\partial/\partial\phi$ and $\partial^2/\partial\phi^2$ as square matrices.

Notice that the potential term $V(\phi)$ in the ϕ-basis is unbounded. Give an estimate on the maximal phase $\phi_{\max}$ needed to describe the first n quantized energy levels of the LC circuit. Moreover, since $V(\phi)$ is unbounded, impose open boundary conditions in the matrix form of $T(\phi)$.

4. Start from the following physical parameters for the LC oscillator:

$$\omega_r/2\pi = 9.375\,\text{GHz}, \qquad Z_r = 25\,\Omega. \tag{15}$$

Take $N_\phi = 2000$ points in the interval $[-\phi_{\max}, \phi_{\max}]$, where to find $\phi_{\max}$ you suppose $n = 20$ energy levels.

Build the matrix for the quantum LC circuit and diagonalize it numerically, obtaining the eigenenergies E_n and the eigenstates $\Psi_n(\phi)$. Plot the potential $V(\phi)$, the first $n = 10$ energy levels ε_n obtained from the Second Quantization procedure, and the first $n = 10$ rescaled wave functions $|\tilde{\Psi}(\phi)|^2 = A|\Psi(\phi)|^2 + E_n$ (being E_n the energies in First Quantization). Take $A = 10^4$ (Since the amplitude of the wave function is very small, you need to amplify them just to visualize them on the plot).

5. We now focus on the transmon qubit in First Quantization. Expand $\hat{n}$ and $\hat{\phi}$ in terms of creation and annihilation operators

$$\hat{\phi} = \left(\frac{2E_C}{E_J}\right)^{1/4} (\hat{b} + \hat{b}^\dagger), \qquad \hat{n} = \frac{i}{2}\left(\frac{E_J}{2E_C}\right)^{1/4} (\hat{b}^\dagger - \hat{b}). \tag{16}$$

Repeat the procedure of the first exercise and write down the Second Quantized form of Eq. (26), upon expanding the cosine potential up to the fourth order in $\hat{\phi}$, and neglecting the counter-rotating terms.

6. First Quantization is particularly advantageous for nonlinear circuit QED system because the nonlinear potential are tipically diagonal in the ϕ-basis. Using the same procedure of Point 3, write the transmon Hamiltonian in the ϕ-basis as $\mathcal{H} = T(\phi) + V(\phi)$ (use again the central difference approximation scheme).

Unlike the harmonic oscillator, the potential $V(\phi)$ is now periodic in ϕ and we can restrict the phase in the interval $[-\pi, \pi]$. Start from the following physical parameters for the transmon qubit:

$$E_C/2\pi = 300\,\text{MHz}, \qquad E_J = 50 \times E_C. \tag{17}$$

Take $N_\phi = 2000$ points in the interval $[-\pi, \pi]$ and remember that periodic boundary conditions must be imposed in the matrix form of $T(\phi)$.

Build the matrix for the transmon qubit and diagonalize it numerically, obtaining the eigenenergies E_n and the eigenstates $\Psi_n(\phi)$. Plot the potential $V(\phi)$, the first $n = 9$ energy levels obtained from the Second Quantized Hamiltonian plus the First Quantized ground state energy, $\varepsilon_n + E_0$ (this fixed a common zero-point energy), and the first $n = 9$ rescaled wave functions $|\tilde{\Psi}(\phi)|^2 = A|\Psi(\phi)|^2 + E_n$ (being E_n the energies in First Quantization). Take $A = 10^4$ as in Point 4.

Discuss the discrepancies between the First and the Second Quantized model.

Solution 3 :

1. Our starting point is the Hamiltonian

$$\hat{H} = \frac{\hat{Q}^2}{2C} + \frac{\hat{\Phi}^2}{2L}. \tag{18}$$

Using the definitions provided in the text, $\hat{n} = \hat{Q}/2$ and $\hat{\phi} = 2\hat{\Phi}$ (since $\hbar = e = 1$) and $E_C = 1/2C$ and $E_L = 1/4L$, one easily arrives at the Hamiltonian

$$\hat{H} = 4E_c\hat{n}^2 + \frac{1}{2}E_L\hat{\phi}^2. \tag{19}$$

2. One has simply to plug the definitions of $\hat{n}$ and $\hat{\phi}$ in terms of creation and annihilation operators in the above Hamiltonian. Some algebra leads to the quantum harmonic oscillator Hamiltonian

$$\hat{H} = \omega_r \left(\hat{a}^\dagger\hat{a} + \frac{1}{2}\right), \tag{20}$$

where $\omega_r = \sqrt{8E_C E_L}$ is the oscillator's resonance frequency. The Hamiltonian is diagonal in Second Quantization and its eigenenergies are $\varepsilon_n = \omega_n\left(n + \frac{1}{2}\right)$.

3. To express the Hamiltonian as a matrix that we can numerically diagonalize obtaining eigenenergies and eigenfunctions, we write the charge number operator in terms of the phase operator as $\hat{n} = -i\partial/\partial\phi$, as suggested in the text. The first-quantized Hamiltonian becomes then

$$\mathcal{H} = -4E_C\frac{\partial^2}{\partial\phi^2} + \frac{1}{2}E_L\phi^2 = T + V(\phi). \tag{21}$$

Now we approximate the first and second derivatives by using the central difference approximation scheme. The first derivative reads

$$\frac{\partial}{\partial\phi}\Psi(\phi) \simeq \frac{\Psi(\phi + \Delta\phi) - \Psi(\phi - \Delta\phi)}{2(\Delta\phi)}. \tag{22}$$

In matrix form this coincides with

$$\frac{\partial}{\partial\phi} \simeq \frac{1}{2(\Delta\phi)} \begin{pmatrix} 0 & 1 & 0 & \cdots & 0 \\ -1 & 0 & 1 & \cdots & 0 \\ 0 & -1 & 0 & \cdots & 0 \\ \vdots & \vdots & \vdots & \ddots & \vdots \\ 0 & 0 & 0 & \cdots & 0 \end{pmatrix}, \tag{23}$$

while the second-order derivative is approximated as

$$\frac{\partial^2}{\partial\phi^2}\Psi(\phi) \simeq \frac{\Psi(\phi-\Delta\phi) - 2\Psi(\phi) + \Psi(\phi+\Delta\phi)}{(\Delta\phi)^2}, \tag{24}$$

and in matrix form we have

$$\frac{\partial^2}{\partial\phi^2} \simeq \frac{1}{(\Delta\phi)^2} \begin{pmatrix} -2 & 1 & 0 & \cdots & 0 \\ 1 & -2 & 1 & \cdots & 0 \\ 0 & 1 & -2 & \cdots & 0 \\ \vdots & \vdots & \vdots & \ddots & \vdots \\ 0 & 0 & 0 & \cdots & -2 \end{pmatrix}. \tag{25}$$

where we imposed open boundary conditions. Clearly, $\Delta\phi$ is the lattice spacing and we assume $\phi \in [-\phi_{\max}, \phi_{\max}]$. The potential term is just a matrix with $E_L\phi^2/2$ on the diagonal and zero elsewhere. We then numerically diagonalize the matrix, assuming N_ϕ points in the interval $[-\phi_{\max}, \phi_{\max}]$. We obtain the eigenvalues E_n and the eigenfunctions $\Psi_n(\phi)$. We numerically compare the eigenvalues obtained from the Hamiltonian in second quantization.

Bear in mind that in order to reproduce the first n energy levels we have to choose $\phi_{\max}$ such that $n\omega_r \simeq E_L\phi_{\max}^2/2$, so $\phi_{\max} = \sqrt{2n\omega_r/E_L}$.

4. Here we provide the Julia code used to realize the First and Second Quantized Hamiltonians for the quantum LC circuit, as well as their numerical diagonalization, and the code used to plot the figure.

```
using QuantumToolbox
using CairoMakie
using SparseArrays
```

```
### THIS FUNCTION CONSTRUCTS THE MATRIX OF A LC CIRCUIT IN FIRST
   QUANTIZATION ###

function LC_matrix(EC, EL, n_level, N_phi)

    # I define the phi variable in the interval [-phi_max, phi_max]
       by taking a grid of 2e3+1 points, and choosing phi_max = sqrt
       (2 * L * omega_r * n) with n=30 energy levels (so accuracy
       more less up to 15 levels)

    phi_max = sqrt(2 * omega_r * n_level / EL)
```

```
    phi = range(-phi_max, phi_max, Int(N_phi))
    Delta_phi = phi[2]-phi[1]

    # I construct the matrix for the n operator

    n =  - 1im/(2 * Delta_phi) * spdiagm(-1 => -ones(size(phi)[1]-1),
        1 => ones(size(phi)[1]-1))

    # I construct the matrix for the kinetic energy

    T = - 4 * EC * 1/Delta_phi^2 .* spdiagm(0 => -2 * ones(size(phi)
       [1]), -1 => ones(size(phi)[1]-1), 1 => ones(size(phi)[1]-1))

    # I construct the matrix for the potential energy

    V = 0.5 * EL * spdiagm(0 => phi.^2)

    # I construct the full Hamiltonian

    H = T + V

    return H, n, phi
end
```

```
# I define the capacitance and inductance variables from the
   resonator frequency and the characteristic impedence

omega_r = 9.375 * 2pi
Z_r = 25

L = Z_r/(omega_r)
C = 1/(Z_r * omega_r)

EC = 1/(2 * C)
EL = 1/(4 * L)

# I compute the eigenenergies and eigenfunctions of the LC circuit in
    first quantization by specifying the number of energy levels (n)
   I want to compute and the flux spacing (N_phi) I want to consider

n_level = 20
N_phi = 2e3
H, n, phi = LC_matrix(EC, EL, n_level, N_phi)
e_r, psi_r = eigen(Qobj(H));
```

```
# I write the resonator Hamiltonian in second quantization to compare
    the energy levels

```

```
N = 500
a = destroy(N)
H = omega_r * (a' * a + 0.5)

e_2, psi_2 = eigen(H);
```

```
# CODE FOR THE FIGURE
fig = Figure(size = (800, 600))

# plot of the potential
ax = Axis(fig[1, 1], title="quantum harmonic oscillator", xlabel="phi
    ", ylabel="E[GHz]/2pi")
V = 0.5 * EL * spdiagm(0 => phi.^2)
lines!(ax, phi, Array(diag(V))/ 2pi, linewidth=2.5)

n_level = 10

# plot of the second quantized energy levels
for j in 1:n_level
    hlines!(ax, e_2[j]/2pi, linewidth=1.5, color="black", linestyle=:
        dash)
end

# plot of the first quantized wave functions
cmap = cgrad(:viridis)
N = Int(round(size(cmap)[1]/n_level, digits=0))-1
colors = [cmap[j*N] for j in 1:n_level]

for j in 1:n_level
    lines!(ax, phi, (abs2.(phi_r[j].data)*1e4 .+ e_r[j])/2pi, color=
        colors[j], linewidth=2)
end

# setting the x- and y-lims
ylims!(e_r[1]/2pi - 10, e_r[n_level]/2pi + 10)
xlims!(-50, 50)

fig
```

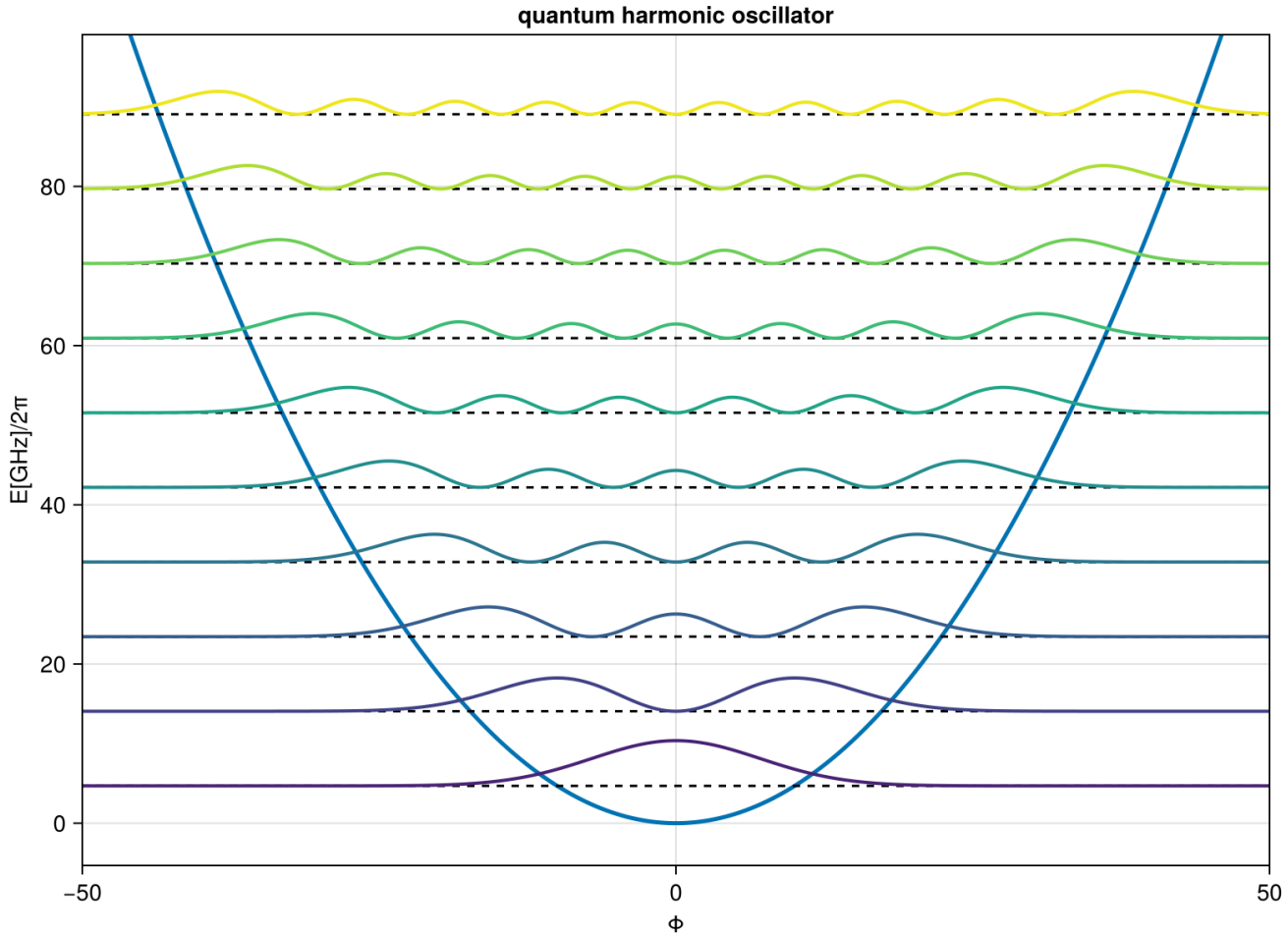

Figure 10: Quantum LC circuit in First Quantization. Harmonic potential (blu solid line), first 10 Second Quantized energy levels (black-dashed lines), first 10 First Quantized rescaled wavefunctions $|\Psi_n(\phi)|^2$, as a function of the phase ϕ.

5. The starting point is now the transmon qubit Hamiltonian

$$\hat{H} = 4E_C\hat{n}^2 - E_J\cos\hat{\phi}. \tag{26}$$

Again, by just plugging the definition of $\hat{n}$ and $\hat{\phi}$, after having expanded the cosine potential to fourth order

$$\cos\hat{\phi} \simeq 1 - \frac{1}{2}\hat{\phi}^2 + \frac{1}{24}\hat{\phi}^4, \tag{27}$$

one arrives, after some algebra, to the Second Quantized Hamiltonian (see also the previous exercise)

$$\hat{H} \simeq \omega_t\hat{b}^\dagger\hat{b} - \frac{E_C}{2}\hat{b}^{\dagger 2}\hat{b}^2, \tag{28}$$

where $\omega_t = \sqrt{8E_CE_J} - E_C$ is the transmon resonance frequency. The Hamiltonian is diagonal in Second Quantization and its eigenenergies are $\varepsilon_n = \omega_t\left(n + \frac{1}{2}\right) - \frac{E_C}{2}n(n-1)$. Differently from the quantum harmonic oscillator, the Second Quantized form of the transmon

Hamiltonian is an approximation, as we expanded the cosine potential and we neglected the counter-rotating terms (whose terms such that $\hat{b}^{\dagger\ell}\hat{b}^{m}$ with $\ell \neq m$).

6. As before, we can write $\hat{n} = -i\partial/\partial\phi$ and the transmon Hamiltonian becomes (we fix $n_g = 0$)

$$\mathcal{H} = -4E_C \frac{\partial^2}{\partial\phi^2} - E_J \cos(\phi) = T + V(\phi). \tag{29}$$

We can proceed as in Point 4 but with an important difference: V is now a periodic function, so periodic boundary conditions must be imposed. The second order derivative becomes

$$\frac{\partial^2}{\partial\phi^2} \simeq \frac{1}{(\Delta\phi)^2} \begin{pmatrix} -2 & 1 & 0 & \cdots & 1 \\ 1 & -2 & 1 & \cdots & 0 \\ 0 & 1 & -2 & \cdots & 0 \\ \vdots & \vdots & \vdots & \ddots & \vdots \\ 1 & 0 & 0 & \cdots & -2 \end{pmatrix}, \tag{30}$$

while the first order derivative reads

$$\frac{\partial}{\partial\Phi} \simeq \frac{1}{2(\Delta\Phi)} \begin{pmatrix} 0 & 1 & 0 & \cdots & -1 \\ -1 & 0 & 1 & \cdots & 0 \\ 0 & -1 & 0 & \cdots & 0 \\ \vdots & \vdots & \vdots & \ddots & \vdots \\ 1 & 0 & 0 & \cdots & 0 \end{pmatrix}. \tag{31}$$

Since the potential is periodic, we restrict the phase interval to $\phi \in [-\pi, \pi]$ and we numerically diagonalize the matrix, assuming N_ϕ points. We numerically compare the eigenvalues obtained from the Hamiltonian in second quantization.

Here we provide the Julia code used to realize the First and Second Quantized Hamiltonians for the transmon qubit, as well as their numerical diagonalization, and the code used to plot the figure.

```
using QuantumToolbox
using CairoMakie
using SparseArrays
```

```
    ### THIS FUNCTION CONSTRUCTS THE MATRIX OF A TRANSMON QUBIT IN
       FIRST QUANTIZATION ###

function transmon_matrix(EC, EJ, N_phi)

    # I define the \phi variable in the interval [-pi, pi] by taking
       a grid of  N   points

    pi = range(-pi, pi, Int(N_pi))
    Delta_phi = phi[2]-phi[1]

```

```
    # I construct the matrix for the n operator

    n = - 1im/(2 * Delta_phi) * spdiagm(-1 => -1 * ones(size(phi)[1]-1), 1 => ones(size(phi)[1]-1))
    n[1, end] = - 1im/(2 * Delta_phi)
    n[end, 1] = + 1im/(2 * Delta_phi)

    # I construct the matrix for the kinetic energy

    T = - 4 * EC * 1/Delta_phi^2 .* spdiagm(0 => -2 * ones(size(phi)[1]), -1 => ones(size(phi)[1]-1), 1 => ones(size(phi)[1]-1))
    T[1, end] = - 4 * EC /Delta_phi^2
    T[end, 1] = - 4 * EC /Delta_phi^2

    # I construct the matrix for the potential energy

    V = -EJ * spdiagm(0 => cos.(phi))

    # I construct the full Hamiltonian

    H = T + V

    return H, n, phi
end
```

```
    # I define also the charging and Josephson energies

    EC = 0.3 * 2pi
    EJ = 50 * EC

    # I compute the eigenenergies and eigenfunctions of the transmon qubit in first quantization by specifying phase spacing (N_phi) I want to consider

    N_phi = 2e3
    H, n, phi = transmon_matrix(EC, EJ, N_phi)
    e_t, psi_t = eigen(Qobj(H));
```

```
    # I write the transmon Hamiltonian in second quantization to compare the energy levels

    N = 30
    omega_t = sqrt(8 * EC * EJ) - EC
    b = destroy(N)
    H = omega_t * b' * b  - 0.5 * EC * b'^2 * b^2

    e_2, psi_2 = eigen(H);
```

```
# CODE FOR THE FIGURE
fig = Figure(size = (800, 600))

# plot of the potential
ax = Axis(fig[1, 1], title="superconducting transmon qubit", xlabel="
    phi", ylabel="E[GHz]/2pi")
V = -EJ * spdiagm(0 => cos.(phi))
lines!(ax, phi, Array(diag(V))/ 2pi, linewidth=2.5)

n_level = 9

# plot of the second quantized energy levels (in the Kerr resonator
    approximation)
for j in 1:n_level
    hlines!(ax, (e_2[j] .+ e_t[1])/2pi, linewidth=1.5, color="black",
        linestyle=:dash)
end

# plot of the first quantized wave functions
cmap = cgrad(:viridis)
N = Int(round(size(cmap)[1]/n_level, digits=0))-1
colors = [cmap[j*N] for j in 1:n_level]

for j in 1:n_level
    lines!(ax, phi, (abs2.(psi_t[j].data) * 1e4 .+ e_t[j])/2pi, color
       =colors[j], linewidth=2)
end

# setting the x- and y-lims
ylims!(e_t[1]/2pi-5, e_t[n_level]/2pi + 5)
xlims!(-pi, pi)

fig
```

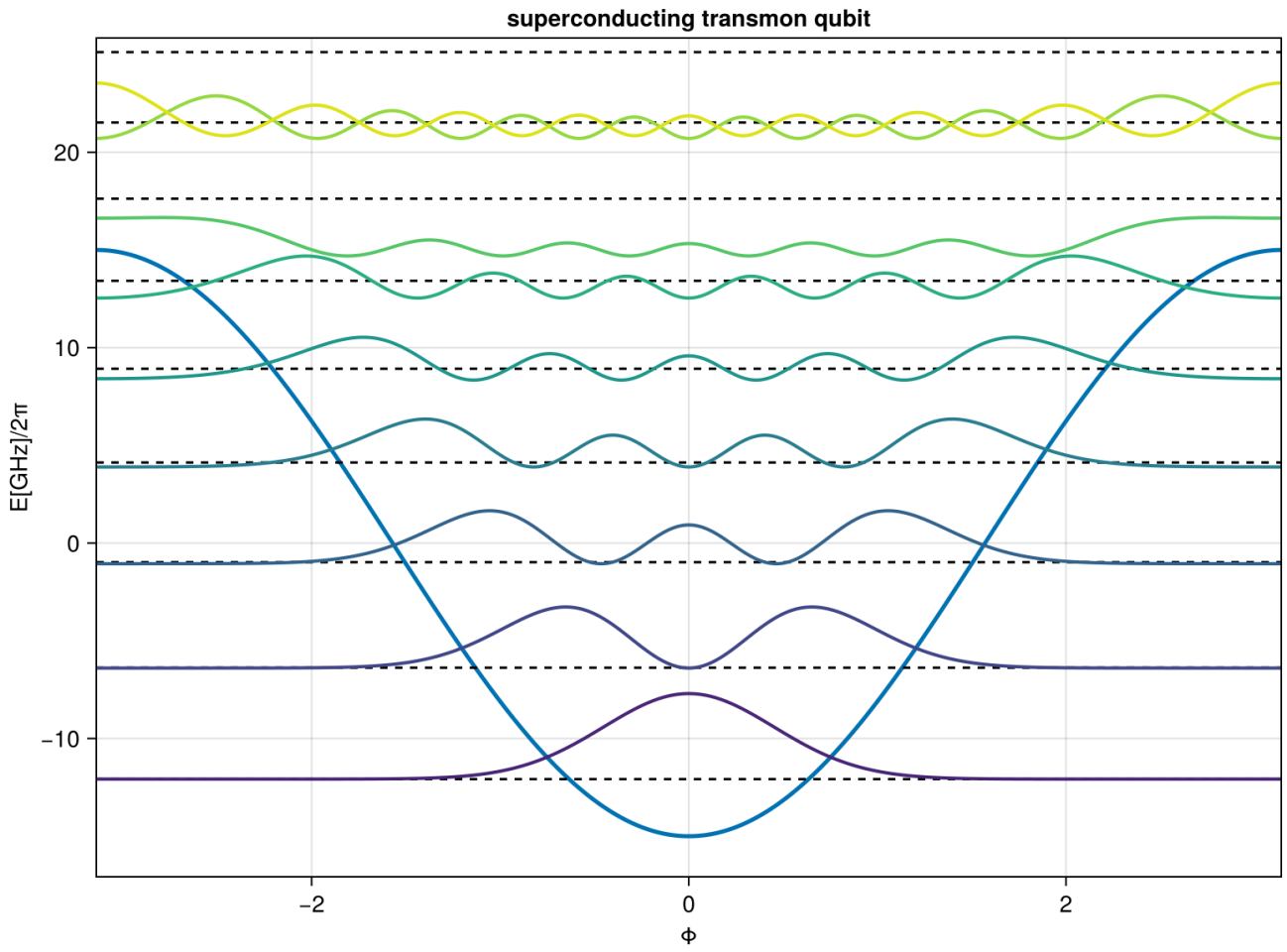

Figure 11: Transmon qubit in First Quantization. Cosine potential (blu solid line), first 9 Second Quantized energy levels (black-dashed lines) plus the First Quantized ground state energy $\varepsilon_n + E_0$, first 9 First Quantized rescaled wavefunctions $|\Psi_n(\phi)|^2$, as a function of the phase ϕ. We notice that for the higher excited states, the Second Quantized Hamiltonian starts deviating from the exact First Quantized Hamiltonian. Moreover, as we go out of the cosine potential well, the two approaches gives completely different results.